PCCP

Accepted Manuscript

ROYAL SOCIETY OF CHEMISTRY

www.rsc.org/pccp

First hyperpolarizability of nitrobenzene in benzene solutions: investigation of the effects of electron correlation within the sequential QM/MM approach

Marcelo Hidalgo Cardenuto[1,2] and Benoît Champagne[1,*]

[1]Laboratoire de Chimie Théorique, Unité de Chimie Physique Théorique et Structurale, University of Namur, rue de Bruxelles, 61, B-5000 Namur, Belgium

[2]Instituto de Física, Universidade de São Paulo, CP 66318, 05314-970 São Paulo, SP Brazil

Abstract

The first hyperpolarizability of nitrobenzene in benzene solutions is evaluated by adopting the sequential-Quantum Mechanics/Molecular Mechanics approach at different correlated wavefunction and density functional theory levels of approximation in order to compare these methods for predicting the solvent effects and in particular the effects of nitrobenzene concentration, which modifies the polarization field due to the surrounding. The liquid configurations are generated using Monte Carlo simulations and the surrounding molecules are represented by point charges, defining an electrostatic embedding. At all levels of approximation, the higher the concentration in nitrobenzene, the larger the first hyperpolarizability of the targeted molecule. At

optical frequencies ($\lambda = 1064\,nm$), for the whole range of concentrations, increasing the amount of Hartree-Fock exchange in the exchange-correlation functional leads to the following observations i) $\beta_{//}$ and β_{HRS} decrease attaining a minimum at the HF level, ii) the octupolar component to β_{HRS} increases, iii) the HRS $\beta_{solv}/\beta_{isol}$ ratio increases, and iv) the EFISHG $\beta_{solv}/\beta_{isol}$ ratio displays a less systematic behavior. Considering the static properties, for which reference CCSD(T) values have been evaluated, M05-2X, LC-BLYP($\mu = 0.33$), and M11 are the most reliable exchange-correlation functionals for predicting both β_{HRS} and its evolution as a function of the nitrobenzene concentration whereas in the case of $\beta_{//}$, these are M05-2X, LC-BLYP($\mu =$ 0.28 and 0.33), and CAM-B3LYP

Keywords: first hyperpolarizability, solvent effects, sequential QM/MM method, electron correlation effects

[0]Electronic addresses: marcelo.hidalgo@unamur.be and benoit.champagne@unamur.be.

1 Introduction

The control and optimization of the nonlinear optical (NLO) properties of molecules is a necessary steps towards designing new compounds and new materials for applications in lasers, optical devices, or data storage [1, 2]. Additional applications can also be foreseen by combining these NLO properties with dynamic properties of molecules, leading to the design of NLO switches, where the NLO properties are triggered by a large range of stimuli [3]. Most NLO-based applications but also characterizations of the NLO properties are carried out in condensed phase (in solutions, crystals, polymer matrices). Therefore, the study of the surrounding effects on the NLO properties has attracted much interest, both theoretically and experimentally. Many approaches and methodologies have been developed to theoretically study the solvent effects, for example, the models of solvent continuum [4–6] and the combined use of quantum mechanics and molecular mechanics (QM/MM) methodologies [7, 8]. The NLO properties of molecules in solutions have been the object of intense investigations [9–24], where successive methodological developments have enabled to better understand solvation effects and to more closely account for experimental observations. Among these, both continuum and QM/MM methodologies were recently used to describe the solvent effects on the first hyperpolarizability (β, which describes, at the molecular level, the second-order NLO effects) contrast of molecular switches [25, 26]. Related techniques are also used to account for in-crystal dressing effects on the hyperpolarizabilities [27–29].

Besides accounting for surrounding effects, the NLO properties are known to be complex quantities to estimate because electron correlation plays an important role. So, for a quantitative prediction of the NLO properties

electron correlation effects must be included. The methods used to include electron correlation are based on wavefunction approaches [30–48] as well as on density functional theory (DFT) [49–76] and many studies have been reported for these different levels of calculation over the last 40 years. In general, Hartree-Fock calculations underestimate the β responses in comparison to correlated perturbation theory and coupled cluster methods in gas phase as well as in solvent [24, 38, 42]. Then, for static properties, second-order Møller-Plesset perturbation theory (MP2) calculations provide generally results in close agreement with reference coupled cluster (CC) calculations whereas, on the other hand, DFT results depend strongly on the functional and particularly on the amount of Hartree-Fock exchange.

In this Paper we investigate the effects of electron correlation on the first hyperpolarizability of nitrobenzene (NB) in benzene (Bzn) solutions of different concentrations. A sequential-QM/MM [77–79] procedure is used to access the liquid configurations using Monte Carlo simulations and then, quantum mechanical calculations are performed for selected snapshots to obtain the first hyperpolarizability. This Paper extents a previous investigation [80], carried out at the time-dependent Hartree-Fock (TDHF) level, where solute-solute interactions have been shown to reduce the first hyperpolarizability as a result of (partial) centro-symmetric arrangements between the nitrobenzene molecules. These calculations have also evidenced that these interactions reduce mostly the dipolar contribution to β whereas the octopular one is little impacted. Here, quantum calculations are performed at different levels of approximation to account for electron correlation effects, DFT and a selection of exchange-correlation functionals as well as molecular orbital-based methods, MP2, CC with singles and doubles (CCSD), and including triple pertubative excitations [CCSD(T)]. Both static and dynamic

first hyperpolarizabilities were evaluated and are compared to results obtained previously at the Hartree-Fock level.

The work is organized as follows: Section 2 describes the key methodological and computational aspects. Section 3 presents and discusses the results and finally the conclusions are drawn in Section 4.

2 Computational procedures

Monte Carlo Simulations

Monte Carlo (MC) simulations were performed in the NPT ensemble (T = 298 K and P = 1 atm) [81] to obtain the liquid structures. These structures represent nitrobenzene in benzene solutions in the given thermodynamic conditions. Different concentrations are obtained by varying the number of NB molecules in the simulation box. The most diluted system is composed by 1 NB + 1000 Bzn molecules and then the number of NB molecules is increased to 20 and 200. The intermolecular interactions are described by the Lennard-Jones potential plus the Coulomb term and the geometries of the molecules are frozen, the geometry of NB having been optimized at the MP2/aug-cc-pVDZ level. The molecular parameters for the solvent are taken from the OPLS force field [82]. The average density determined during the simulations are $0.875 \pm 0.005\, g/cm^3$ for the most dilute case and 0.883 ± 0.005 and $0.938 \pm 0.005\, g/cm^3$ when there are 20 and 200 nitrobenzene molecules, respectively. The radial distribution function [81] is calculated and gives structural information related to the solvation shells as well as the limits (size) of these shells. In a MC simulation of liquids the number of molecular configurations accessible is very large. Considering all these configurations is computationally not feasible and a reduced number

of statistically-uncorrelated configurations has to be selected for the purpose of the ab initio calculations [78, 79].

ab initio calculations

Following the MC simulations quantum mechanical calculations are performed using statistically-uncorrelated configurations (snapshots). The first hyperpolarizability of nitrobenzene is calculated in an electrostatic embedding that describes the solvent effects. Each atom of the solvent molecules - as well as of the other solute molecules - is described by a point charge. Both static and dynamic ($\lambda = 1064nm$) first hyperpolarizabilities are evaluated at the DFT level, using the time-dependent Kohn-Sham and coupled-perturbed Kohn-Sham (CPKS) methods, respectively. The following hybrid and long-range corrected exchange-correlation DFT functionals were selected: BLYP, combining the Becke exchange functional [83] and Lee-Yang-Parr correlation functional [84], the hybrid B3LYP [85], M05 [86], M05-2X [87], and M11 [88] from Minnesota, and the long-range corrected CAM-B3LYP [89] and LC-BLYP [90]. These functionals have been used in several investigations of (hyper)polarizabilities. For instance, in a recent study [42] LC-BLYP was shown to provide better β values for push-pull π-conjugated chains than B3LYP and BLYP, when compared to CCSD(T). Moreover, a study pointed out that CAM-B3LYP improves B3LYP β estimatives of long polymethineimine oligomers [60]. Similarly, in a study on push-pull π-conjugated molecules [58], the long-corrected LC scheme applied to the BOP functional (LC-BOP) was demonstrated to better perform than B3LYP to estimate their first hyperpolarizabilities.

These XC functionals differ in particular by the amount of Hartree-Fock

exchange, 20%, 26%, and 52%, for B3LYP, M05, and M05-2X, whereas M11, CAM-B3LYP, and LC-BLYP are range-separated hybrids where the amount of HF exchange goes from 42.8, 19 and 0%, in the short-range, to 100, 65, and 100 % in the long-range, respectively. In range-separated hybrids, the transition between the short- and long-range regions is dictated by the range-separated parameter, μ. The larger $1/\mu$, the more DFT exchange is included in the functional. The standard μ values for CAM-B3LYP and M11, 0.33 and 0.25 were adopted in this study, respectively. For LC-BLYP, different μ values were tested: the standard 0.47 and 0.33 values as well as a smaller value of 0.15. Then, following the procedure described in Refs. [91,92] a physically-motivated μ value was used. It was determined so as to reproduce as closely as possible Koopmans' theorem for the neutral system [IE(N) = E(N-1)-E(N) = -ϵ_{HOMO}(N), with IE the ionization energy, E the total electronic energy, N the number of electrons of the neutral system, and HOMO the highest occupied molecular orbital]. The best value was found to be 0.28, slightly smaller than the original μ value [90]. Several studies have indeed shown that the best IE-tuned μ value gets smaller with the extension of the π-conjugated system [68,73,74].

At the MP2, CCSD, and CCSD(T) levels, only the static properties were evaluated. This is done using the finite field (FF) procedure [93], where the energy is calculated for different amplitudes of the external electric field and the successive energy derivatives with respect to the field are calculated numerically. To improve and control the accuracy on the numerical derivatives, the Romberg procedure is used [94,95]. It allows to diminish the effects of higher-order contaminations. Field amplitudes from $\pm$ 0.0004 to $\pm$ 0.0064 a.u. in a geometric progression ratio of 2 were used. To achieve high accuracy on the third-order energy derivatives, the convergence on the SCF (HF

and DFT) energy was lowered to 10^{-11} a.u. whereas to 10^{-9} in the CCSD and CCSD(T) iterative procedures. This allows to reach an accuracy on β of 0.01 a.u or better as could be estimated from the comparison of static DFT values obtained, on one side, using the analytical CPKS method and, on the other side, the corresponding numerical differentiation scheme. In all β calculations the 6-31+G(d) basis set were used.

In this work the following quantities were calculated : β_{HRS}, $\beta_{//}$, $|\beta_{J=1}|$, $|\beta_{J=3}|$, DR, and ρ. $\beta_{//}$ is the projection of the vector part of β on the dipole moment μ:

$$\beta_{//} = \frac{1}{5} \sum_{\zeta}^{x,y,z} \frac{\mu_\zeta}{||\vec{\mu}||} \sum_{\eta}^{x,y,z} (\beta_{\zeta\eta\eta} + \beta_{\eta\zeta\eta} + \beta_{\eta\eta\zeta}) = \frac{3}{5} \sum_{\zeta}^{x,y,z} \frac{\mu_\zeta \beta_\zeta}{||\vec{\mu}||}$$

which can be retrieved from electric-field-induced second harmonic generation experiment. The β_{HRS} and the other related quantities are associated with hyper-Rayleigh scattering (HRS) experiments and with the intensity of the vertically-polarized (along the Z axis) signal scattered at 90° with respect to the propagation direction (Y axis) for a non-polarized incident light beam, which can be decomposed in two ways:

$$\begin{aligned} \langle \beta_{HRS}^2 \rangle &= \langle \beta_{ZZZ}^2 \rangle + \langle \beta_{ZXX}^2 \rangle \\ &= [1 + DR] \langle \beta_{ZZZ}^2 \rangle \\ &= \frac{10}{45} |\beta_{J=1}|^2 + \frac{10}{105} |\beta_{J=3}|^2 \\ &= \left(\frac{2}{9} + \frac{2}{21} \rho^2 \right) |\beta_{J=1}|^2 \end{aligned}$$

$\langle \beta_{ZZZ}^2 \rangle$ and $\langle \beta_{ZXX}^2 \rangle$ are the β tensor orientational averages, which are pro-

portional to the scattered signal intensity for vertically- and horizontally-polarized incident light beams, respectively. Their ratio is known as the depolarization ratio (DR) and depends on the shape of the NLOphore. The β tensor can also be decomposed as the sum of a dipolar (J=1) and an octupolar (J=3) tensorial β_J-component, which can be used to express β_{HRS}. The ratio of these components, $\rho = |\beta_{J=3}|/|\beta_{J=1}|$ is known as the nonlinear anisotropy. Detailed expressions of $\langle\beta^2_{ZZZ}\rangle$, $\langle\beta^2_{ZXX}\rangle$, $|\beta_{J=1}|^2$ and $|\beta_{J=3}|^2$ are available in [24]. All reported β values are given in atomic units (1 au of $\beta = 3.63\,10^{-42}\,m^4\,V^{-1} = 3.2063\,10^{-53}\,C^3\,m^3\,J^{-2} = 8.641\,10^{-33}\,esu$) and expressed within the T convention.

In our previous work [80], the first hyperpolarizabilities were reported as statistically-converged averages over 100 configurations together with their standard deviations, describing the broadening of the values. Here the results are obtained in one calculation performed in an averaged solvent electrostatic configuration (ASEC) [96] composed by all these 100 configurations. Since this is the first time the ASEC approach is employed for calculating hyperpolarizabilities, its performance with respect to the conventional approach, reporting statistically-converged averages and their standard deviations, is assessed.

The classical Monte Carlo simulations were performed with the DICE program [97], the quantum mechanics calculations with Gaussian09 program [98] whereas the Romberg scheme was carried out with a locally-developed program.

3 Results

DFT dynamic first hyperpolarizabilities

The geometry of NB was optimized at MP2 level and the Dunning's correlation-consistent aug-cc-pVDZ basis set. The NB atomic charges needed for the MC simulations were calculated using the electrostatic potential fitting scheme CHELPG [99]. Both geometry and atomic charges were evaluated in the presence of solvent (benzene) within the polarizable continuum model PCM.

The first hyperpolarizability was calculated using a set of 100 configurations generated in the MC simulations. Analyzing the RDF function allows to highlight a region, which ranges from the reference NB up to 18 Å of radius. This comprises the first, second, and third solvation shells around the NB for a total of 195 molecules. Looking at the first solvation shell, the number of NB molecules goes from 1 in the most dilute case up to four in the most concentrated one. All molecules are treated as point charges (PC).

Tables 1 to 3 present the dynamic hyperpolarizabilities calculated with the different XC functionals (HF is also shown) and for crescent concentrations. The solvent effects are described using the ASEC scheme, where the PC values are averages over the selected 100 snapshots. Then, Table 4 compares these ASEC values to those obtained as the averages over 100 calculations with their standard deviations. In figure 2, β_{HRS} and $\beta_{//}$ are plotted as a function of the number of NB molecules in the box, as well as their ratios with respect to the gas phase, in vacuo, or isolated values. Note that in this sub-section only the Gaussian09 $\mu = 0.47$ default LC-BLYP value was considered. The solvent effects as described at both types of levels of calculations (HF and DFT) show the same trend, an increase of β_{HRS} and $\beta_{//}$ with respect to the isolated molecule. Moreover, as the number of NB

molecules increases, the surrounding gets more polar, which increases the polarization field, and thereof the dielectric constant of the medium. This causes a further enhancement in the β_{HRS} values. The inclusion of electron correlation leads to larger values of the first hyperpolarizability in comparison to the HF results, independent of the XC functional considered. All β quantities increase consistently according to the sequence TDHF $<$ LC-BLYP($\mu = 0.47$) $<$ M11 $<$ M05-2X $<$ CAM-B3LYP $<$ B3LYP $<$ M05 $<$ BLYP, which to some extent follows the order of decreasing amount of HF exchange. With the exception of M05-2X, note that DR - and subsequently ρ since it evolves in the opposite direction - follows the same ordering. This corresponds to an increase of the octupolar component of β when decreasing the amount of HF exchange. Though β increases by incorporating electron correlation at the DFT level, the $\beta_{solv}/\beta_{isol}$ ratios are larger at the HF level for the $\beta_{//}$ quantities whereas for β_{HRS} the HF $\beta_{solv}/\beta_{isol}$ ratios are rather small and of the same amplitude as with BLYP and M05.

Comparison between the ASEC and conventional schemes demonstrates the adequacy of the former. Indeed, the differences between the β values are of the order of 1 a.u., i.e. less than one percent whereas similar correspondance is achieved for DR and ρ. This allows taking advantage of the ASEC scheme when employing MO-based correlated methods, since these are computationally much more demanding.

Table 1: Dynamic ($\lambda = 1064\,nm$) first hyperpolarizability (a.u.) of nitrobenzene in benzene as determined with TDHF and TDDFT for different XC functionals. The solvent molecules are described by point charges. These values correspond to the case with 1 NB + 1000 Bzn in MC simulation and have been evaluated within the ASEC scheme.

	TDHF [80]	LC-BLYP($\mu = 0.47$)	M11	M05-2X	CAM-B3LYP	B3LYP	M05	BLYP
β_{HRS}	163.26	215.08	221.45	238.92	277.74	355.02	374.96	433.28
$\beta_{//}$	144.19	263.53	277.47	289.40	350.06	458.43	495.84	571.21
$\beta_{J=1}$	189.77	344.44	362.68	379.30	458.57	602.13	650.45	752.89
$\beta_{J=3}$	442.51	457.05	456.05	513.51	565.08	690.93	699.31	805.30
DR	2.23	3.37	3.52	3.31	3.58	3.80	4.02	4.03
ρ	2.33	1.33	1.26	1.35	1.23	1.15	1.08	1.07

Table 2: Dynamic ($\lambda = 1064\,nm$) first hyperpolarizability (a.u.) of nitrobenzene in benzene as determined with TDHF and TDDFT for different XC functionals. The solvent molecules are described by point charges. The values correspond to the case with 20 NB + 1000 Bzn in MC simulation and have been evaluated within the ASEC scheme.

	TDHF [80]	LC-BLYP($\mu = 0.47$)	M11	M05-2X	CAM-B3LYP	B3LYP	M05	BLYP
β_{HRS}	169.83	224.80	231.18	249.51	289.64	369.30	389.11	450.34
$\beta_{//}$	156.39	279.16	292.77	306.64	369.09	481.14	518.26	598.52
$\beta_{J=1}$	205.64	364.75	382.60	401.74	483.36	631.84	679.75	788.76
$\beta_{J=3}$	451.86	469.22	468.64	526.38	579.40	707.44	715.31	823.28
DR	2.31	3.46	3.60	3.40	3.67	3.88	4.09	4.12
ρ	2.20	1.29	1.22	1.31	1.20	1.12	1.05	1.04

Table 3: Dynamic ($\lambda = 1064\,nm$) first hyperpolarizability (a.u.) of nitrobenzene in benzene as determined with TDHF and TDDFT for different XC functionals. The solvent molecules are described by point charges. The values correspond to the case with 200 NB + 1000 Bzn in MC simulation and have been evaluated within the ASEC scheme.

	TDHF [80]	LC-BLYP($\mu = 0.47$)	M11	M05-2X	CAM-B3LYP	B3LYP	M05	BLYP
β_{HRS}	179.70	239.32	245.47	265.28	307.45	390.54	410.45	475.75
$\beta_{//}$	174.56	302.41	314.96	332.00	397.41	514.73	551.93	638.86
$\beta_{J=1}$	229.32	394.99	411.49	434.79	520.29	675.80	723.77	841.80
$\beta_{J=3}$	465.13	487.20	487.45	545.72	600.71	731.99	739.37	850.33
DR	2.43	3.58	3.70	3.53	3.78	3.99	4.19	4.23
ρ	2.03	1.23	1.18	1.26	1.15	1.08	1.02	1.01

Table 4: Dynamic ($\lambda = 1064\,nm$) first hyperpolarizability (a.u.) of nitrobenzene in benzene as determined with TDHF and different functionals. The solvent molecules are described by point charges. The values correspond to the case with 1 NB + 1000 Bzn in MC simulation. This table compares the results obtained a) using an averaged configuration of point charges, determined from 100 configurations, which corresponds to the ASEC scheme and b) using 100 solvent configurations, where the reported values are the averages and their standard deviations.

	TDHF	LC-BLYP($\mu = 0.47$)	M11	M05-2X	CAM-B3LYP	B3LYP	M05	BLYP
β_{HRS}	163.26	215.08	221.45	238.92	277.74	355.02	374.96	433.28
	163.83 ±14.02	215.51 ± 20.55	222.18 ± 21.25	239.22 ± 22.25	278.08 ± 25.20	355.15 ± 30.18	374.71 ± 30.09	433.00 ± 35.87
$\beta_{//}$	144.19	263.53	277.47	289.40	350.06	458.43	495.84	571.21
	143.76 ± 25.90	263.52 ± 32.54	278.03 ± 32.63	288.94 ± 35.74	349.90 ± 39.73	457.94 ± 47.43	494.36 ± 47.22	569.97 ± 56.66
$\beta_{J=1}$	189.77	344.44	362.68	379.30	458.57	602.13	650.45	752.89
	190.13 ± 33.43	344.71 ± 42.27	363.60 ± 42.50	379.05 ± 46.48	458.70 ± 51.77	601.94 ± 62.06	649.00 ± 61.75	751.82 ± 74.54
$\beta_{J=3}$	442.51	457.05	456.05	513.51	565.08	690.93	699.31	805.30
	443.18 ± 23.30	458.04 ± 29.38	457.30 ± 30.80	514.60 ± 31.19	565.89 ± 34.65	691.36 ± 39.58	700.44 ± 38.42	805.23 ± 43.62
DR	2.23	3.37	3.52	3.31	3.58	3.80	4.02	4.03
	2.23 ± 0.18	3.35 ± 0.20	3.51 ± 0.17	3.30 ± 0.20	3.57 ± 0.19	3.79 ± 0.18	4.00 ± 0.17	4.02 ± 0.19
ρ	2.33	1.33	1.26	1.35	1.23	1.15	1.08	1.07
	2.39 ± 0.35	1.34 ± 0.10	1.27 ± 0.08	1.37 ± 0.10	1.24 ± 0.08	1.16 ± 0.07	1.08 ± 0.06	1.08 ± 0.06

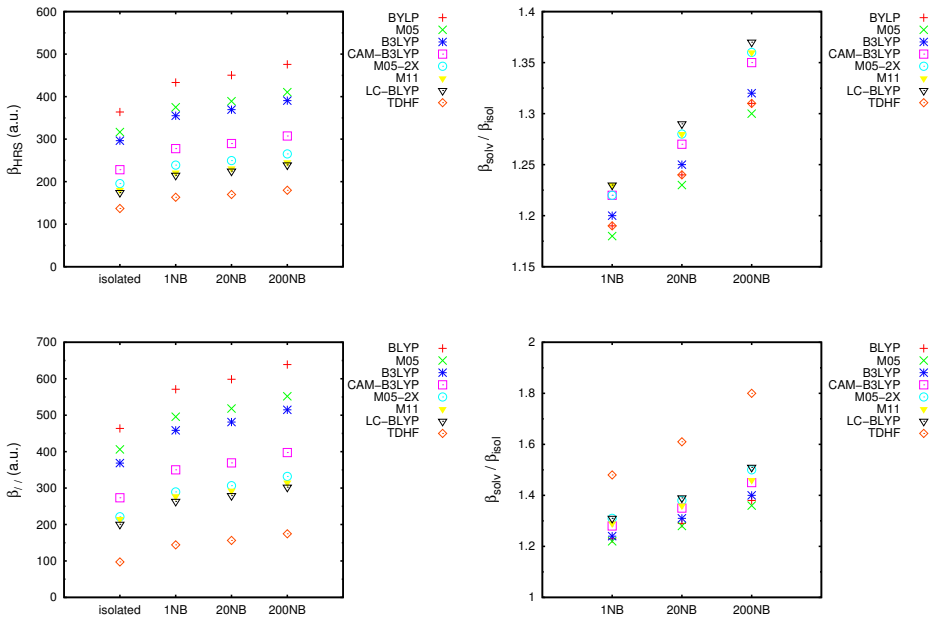

Figure 1: Dynamic (1064 *nm*) first hyperpolarizability of nitrobenzene in benzene solutions obtained at the TDDFT and TDHF levels. Top) β_{HRS} and the corresponding solvated/in vacuo ratios; bottom) $\beta_{//}$ and the corresponding solvated/in vacuo ratios. Solvent molecules are represented by point charges and solvent effects described within the ASEC scheme.

DFT versus wavefunction static first hyperpolarizabilities

The static first hyperpolarizabilities and the β_{solv} / β_{isol} ratios are gathered in Table 5 for β_{HRS} and in Table 6 for $\beta_{//}$. Within the iterative Romberg procedure, a range of field amplitudes from ± 0.0004 to ± 0.0064 a.u. leads to a total of 100 single-point energy calculations to obtain all the first hyperpolarizability tensor components at the MP2, CCSD, and CCSD(T) levels of approximation. For an intermediate concentration of 20 NB in Bzn, the numerical accuracy was tackled. So, using the CPHF scheme, β_{HRS} amounts to

128.760 a.u. while the FF/HF scheme with Romberg's iteration gives 128.762 a.u.. Similar negligible differences are observed for calculations considering the isolated molecule as well as other concentrations. These FF calculations are performed using an averaged solvent configuration composed by 100 solvent configurations. These averaged configurations allow to use just one calculation for each field amplitude considered, which is particularly advantageous from the computational point of view for correlated wavefunction calculations. For LC-BLYP calculations, in addition to the default $\mu = 0.47$ value, range-separated parameters of 0.15, 0.28 (tuned to best reproduce the first ionization energy), and 0.33 were also considered.

As shown in Table 5, the MP2 β_{HRS} values are larger than those evaluated at the CCSD and CCSD(T) levels. The CCSD values are typically 10% smaller than the CCSD(T) ones whereas MP2 overestimates the latter by 15%. In fact, without considering μ in LC-BLYP, the CCSD β_{HRS} values are bracketed by the HF and LC-BLYP($\mu = 0.47$) results, the CCSD(T) ones by M11 and M05-2X and finally CAM-B3LYP and B3LYP bracket the MP2 results (except for the isolated molecule where the β_{HRS} ordering is M05-2X $<$ MP2 $<$ CAM-B3LYP). These relative amplitudes of the β values as a function of the method are typical of what was already observed for other push-pull π-conjugated compounds. To assess the solvent effects as described by the different levels of approximation and functionals we now consider the $\beta_{solv}/\beta_{isol}$ ratios in addition to the absolute values. First, the CCSD(T) $\beta_{solv}/\beta_{isol}$ ratios are most closely reproduced by the CCSD and then by the MP2 method. Turning to the DFT levels, among the XC functionals the best agreement on the $\beta_{solv}/\beta_{isol}$ ratio is achieved with LC-BLYP($\mu = 0.47$) and M11 while M11 is slightly preferential because it provides closer agreement on the absolute β values. The next XC functionals to provide accu-

rate $\beta_{solv}/\beta_{isol}$ ratios are M05-2X and CAM-B3LYP, with a preference for M05-2X since the absolute β values are better reproduced. The other XC functionals with smaller amounts of HF exchange further overestimate the β values and underestimates the $\beta_{solv}/\beta_{isol}$ ratios. Interestingly, the HF method underestimates both the β values and the $\beta_{solv}/\beta_{isol}$ ratios. Then, the μ parameter was successively decreased from 0.47 to 0.15, increasing the amount of DFT exchange. A $\mu = 0.33$ value provides the best agreement with the CCSD(T) β_{HRS} values of nitrobenzene when it is solvated whereas it is $\mu = 0.47$ for the isolated species. For $\mu = 0.33$ and 0.47 the $\beta_{solv}/\beta_{isol}$ ratio is underestimated by 5-8%. Further reduction of $\mu =$ leads to overestimated β_{HRS} responses whereas $\beta_{solv}/\beta_{isol}$ ratio remains underestimated. Therefore, the IE-tuned $\mu =$ value does not lead to improved results with respect to the default value(s).

In the case of $\beta_{//}$, the performances of the different DFT XC functionals with respect to CCSD(T) are, to a large extent, similar to those observed for β_{HRS}. Moreover, the CCSD values are typically 13% smaller than the CCSD(T) ones whereas MP2 overestimates the latter by 20%. Besides for the isolated species, the CCSD(T) $\beta_{//}$ values are bracketed by the M05-2X and CAM-B3LYP results. On the other hand, the CCSD and LC-BLYP($\mu =$ 0.47) values are very similar while the MP2 results are inbetween the CAM-B3LYP and B3LYP results. The corresponding CCSD(T) $\beta_{solv}/\beta_{isol}$ ratios range from 1.42 for 1NB to 1.69 for 200NB. Like for β_{HRS} the closest results are obtained with CCSD but now functionals with a large amount of HF exchange overcome MP2. In fact, the larger the amount of HF exchange, the closer the DFT $\beta_{solv}/\beta_{isol}$ ratio with respect to CCSD(T). Considering both the absolute $\beta_{//}$ values and the $\beta_{solv}/\beta_{isol}$ ratios, CAM-B3LYP and M05-2X are efficient functionals to reproduce the CCSD(T) results. In addition, HF

is behaving differently, underestimating $\beta_{//}$ but overestimating $\beta_{solv}/\beta_{isol}$. Then, when increasing the amount of DFT exchange in LC-BLYP via a reduction of μ an improved agreement is observed with the CCSD(T) $\beta_{//}$ values. This is the case for $\mu = 0.28$ and 0.33 but not for 0.15.

Table 5: Static β_{HRS} (a.u.) of nitrobenzene in benzene solutions as obtained at different levels of approximation together with their ratios with respect to the isolated molecule values, β_{solv} / β_{isol}.

	isolated	1NB	$\frac{\beta_{solv}}{\beta_{isol}}$	20NB	$\frac{\beta_{solv}}{\beta_{isol}}$	200NB	$\frac{\beta_{solv}}{\beta_{isol}}$
HF	105.40	124.10	1.18	128.76	1.22	135.80	1.29
CCSD(T)	123.06	159.89	1.30	168.73	1.37	183.06	1.49
CCSD	113.82	145.58	1.28	153.78	1.35	166.01	1.49
MP2	145.38	183.74	1.26	193.03	1.33	207.06	1.42
BLYP	198.90	237.13	1.19	246.35	1.24	260.35	1.31
M05	189.57	224.41	1.18	232.93	1.23	245.69	1.30
B3LYP	182.00	217.54	1.20	226.09	1.24	238.96	1.31
CAM-B3LYP	151.05	183.54	1.22	191.30	1.27	203.01	1.34
M05-2X	135.87	165.29	1.22	172.40	1.27	183.06	1.35
M11	122.91	151.44	1.23	158.18	1.29	168.28	1.37
LC-BLYP ($\mu = 0.47$)	122.47	150.81	1.23	157.58	1.29	167.77	1.37
LC-BLYP ($\mu = 0.33$)	133.75	165.29	1.24	172.76	1.29	184.15	1.38
LC-BLYP ($\mu = 0.28$)	141.16	174.12	1.23	181.90	1.29	193.83	1.37
LC-BLYP ($\mu = 0.15$)	170.49	206.97	1.21	215.65	1.26	229.04	1.34

Table 6: Static $\beta_{//}$ (a.u.) of nitrobenzene in benzene solutions as obtained at different levels of approximation together with their ratios with respect to the isolated molecule values, β_{solv} / β_{isol}.

	isolated	1NB	$\frac{\beta_{solv}}{\beta_{isol}}$	20NB	$\frac{\beta_{solv}}{\beta_{isol}}$	200NB	$\frac{\beta_{solv}}{\beta_{isol}}$
HF	56.24	92.07	1.64	101.47	1.80	115.56	2.05
CCSD(T)	138.90	197.36	1.42	211.82	1.52	235.34	1.69
CCSD	118.66	169.97	1.43	183.78	1.55	204.16	1.72
MP2	181.68	240.11	1.32	254.84	1.40	277.10	1.53
BLYP	223.51	285.00	1.26	300.61	1.34	324.10	1.45
M05	217.99	273.05	1.25	287.15	1.32	308.03	1.41
B3LYP	203.61	259.73	1.28	273.97	1.35	295.21	1.45
CAM-B3LYP	162.93	214.53	1.32	227.47	1.40	246.86	1.52
M05-2X	140.49	187.70	1.34	199.68	1.42	217.39	1.55
M11	129.32	174.44	1.35	185.58	1.44	202.00	1.56
LC-BLYP ($\mu = 0.47$)	126.21	171.46	1.39	182.79	1.45	199.74	1.58
LC-BLYP ($\mu = 0.33$)	141.92	192.38	1.36	204.94	1.44	223.90	1.58
LC-BLYP ($\mu = 0.28$)	150.80	203.64	1.35	216.79	1.44	236.71	1.57
LC-BLYP ($\mu = 0.15$)	184.75	243.73	1.32	258.60	1.40	281.19	1.52

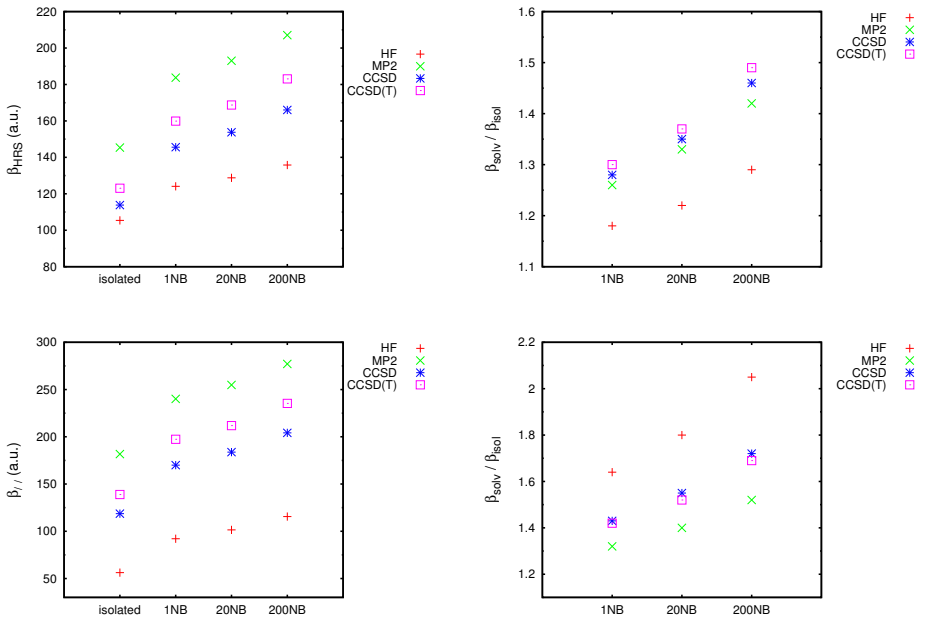

Figure 2: Static first hyperpolarizability of nitrobenzene in benzene solutions obtained at the MP2, CCSD, and CCSD(T) levels (as well as the HF values). Top) β_{HRS} and the corresponding solvated/isolated ratios; bottom) $\beta_{//}$ and the corresponding solvated/isolated ratios. Solvent molecules are represented by point charges and solvent effects described within the ASEC scheme.

4 Conclusions, and outlook

In this article the first hyperpolarizability of nitrobenzene in benzene solutions has been evaluated by adopting the sequential-QM/MM approach at different correlated wavefunction and density functional theory levels of approximation. The objective was to compare these methods for predicting the solvent effects and in particular the effects of nitrobenzene concentration, which modifies the polarization field due to the surrounding. These concentration variations are achieved by tuning the number of nitrobenzene molecules from 1 to 20, and to 200 in an environment of 1000 benzene solvent molecules. In this approach the liquid configurations are generated using Monte Carlo simulations and the surrounding molecules are represented by point charges, defining an electrostatic embedding.

All the β calculations have been carried out with the 6-31+G(d) basis set. Though this choice is substantiated by previous studies, including [42], additional CCSD(T) calculations were performed with the aug-cc-pVDZ basis set for 1NB solvated by 1000 benzene molecules. The corresponding β_{HRS}, $\beta_{//}$, and DR values amount to 157.55 a.u., 197.22 a.u., and 3.43 in comparison to the 6-31+G(d) values of 159.89 a.u., 197.38 a.u., and 3.34, respectively.

At all levels of approximation, the higher the concentration in nitrobenzene, the larger the first hyperpolarizability of the targeted molecule. At optical frequencies ($\lambda = 1064\,nm$), for the whole range of concentrations, when increasing the amount of Hartree-Fock exchange in the exchange-correlation functional, the following trends are observed i) the EFISHG ($\beta_{//}$) and HRS (β_{HRS}) first hyperpolarizabilities decrease attaining a minimum at the HF level, ii) the octupolar component to β_{HRS} increases, iii) the HRS $\beta_{solv}/\beta_{isol}$ ratio increases, iv) the EFISHG $\beta_{solv}/\beta_{isol}$ ratio displays a less systematic be-

havior, and v) the TDHF method gives among the smallest HRS $\beta_{solv}/\beta_{isol}$ ratios but the largest EFISHG $\beta_{solv}/\beta_{isol}$ ones. Turning to static properties, for which reference CCSD(T) values have been evaluated, M05-2X, LC-BLYP(μ = 0.33), and M11 are the most reliable exchange-correlation functionals for predicting both β_{HRS} and its evolution as a function of the nitrobenzene concentration. Note that concentration effects are still better described at the MP2 and CCSD levels, though the β_{HRS} amplitudes are overestimated/underestimated by 15 and 10 %, respectively. In the case of $\beta_{//}$, M05-2X, LC-BLYP(μ = 0.28 and 0.33), and CAM-B3LYP are the most efficient functionals to reproduce both its amplitude and its evolution as a function of the nitrobenzene concentration. So, the IE-tuned ranged-separated hybrid performs well for $\beta_{//}$ and slightly less for β_{HRS} and their solvation ratios. This complements recent studies with contrasted results on the performance of IE-tuned range-serarated hybrids for evaluating (hyper)polarizabilities of π-conjugated systems [68, 73, 74].

Acknowledgement

M. H. C. acknowledges the CNPq (Brazil) and the University of São Paulo for his postdoctoral grant as well as the Belgian Government (IUAP No P7/5 "Functional Supramolecular Systems") for financial support. This work is supported by funds from the Belgian Government (IUAP No P7/5) and the Francqui Foundation. The calculations were performed on the computers of the Consortium des Équipements de Calcul Intensif and mostly those of the Technological Platform of High-Performance Computing, for which we gratefully acknowledge the financial support of the FNRS-FRFC (Conventions No. 2.4.617.07.F and 2.5020.11) and of the University of Namur.

References

[1] P. N. Prasad and D. J. Willians, *Introduction to Nonlinear Optical Effects in Molecules and Polymers*, Wiley Interscience, New York, 1991.

[2] M. G. Papadopulos, A. J. Sadlej, and J. Leszcczynski, *Non-linear Optical Properties of Matter - From Molecules to Condensed Phases*, Springer, Dordrecht, 2006.

[3] F. Castet, V. Rodriguez, J. -L. Pozzo, L. Ducasse, A. Plaquet, and B. Champagne, *Acc. Chem. Res.*, 2013, **46**, 2656.

[4] J. Tomasi, *Theor Chem Acc*, 2004, **112** 184.

[5] J. Tomasi, B. Mennucci, R. Cammi, *Chem. Rev.*, 2005, **105**, 2999.

[6] R. Cammi, M. Cossi, and J. Tomasi, *J. Chem. Phys.* 1996, **104**, 4611.

[7] A. Warshel and M. Levitt, *J. Mol. Biol.*, 1976, **103**, 227.

[8] J. Gao, *Reviews in Computational Chemistry*, VCH, New York, 1996, p. 119.

[9] J. Yu and M. C. Zerner, *J. Chem. Phys.*, 1994, **100**, 7487.

[10] K. V. Mikkelsen, Y. Luo, H. Ågren, P. Jørgensen, *J. Chem. Phys.*, 1994, **100**, 8240.

[11] S. Di Bella, T. J. Marks, and M. A. Ratner, *J. Am. Chem. Soc.*, 1994, **116**, 4440.

[12] C. Dehu, F. Meyers, E. Hendrickx, K. Clays, A. Persoons, S. A. Marder, and J. L. Brédas, *J. Am. Chem. Soc.*, 1995, **117**, 10127.

[13] R. Cammi, B. Mennucci, and J. Tomasi, *J. Am. Chem. Soc.*, 1998, **120**, 8834.

[14] P. Macak, P. Norman, Y. Luo, and H. Ågren, *J. Chem. Phys.*, 2000, **112**, 1868.

[15] W. Bartkowiak, R. Zalesny, W. Niewodniczanski, and J. Leszcynski, *J. Phys. Chem. A*, 2001, **105**, 10702.

[16] P. C. Ray and J. Leszczynski, *Chem. Phys. Lett.*, 2004, **399**, 162.

[17] J. Kongsted, A. Anders, K. V. Mikkelsen, and O. Christiansen, *J. Chem. Phys.*, 2004, **120**, 3787.

[18] L. Jensen and P.Th. van Duijnen, *J. Chem. Phys.*, 2005, **123**, 074307.

[19] H. Reis, A. Grzybowski, and M. G. Papadopoulos, *J. Phys. Chem. A*, 2005, **109**, 10106.

[20] L. Ferrighi, L. Frediani, C. Cappelli, P. Salek, H. Ågren, T. Helgaker, and K. Ruud, *Chem. Phys. Lett.*, 2006, **425**, 267.

[21] C. B. Nielsen, O. Christiansen, K. V. Mikkelsen, and J. Kongsted, *J. Chem. Phys.*, 2007, **126**, 154112.

[22] Y. Takimoto, C.M. Isborn, B. E. Eichinger, J. J. Rehr, and B. H. Robinson, *J. Phys. Chem. C*, 2008, **112**, 8016.

[23] S.I. Lu, C.C. Chiu and Y.F. Wang, *J. Chem. Phys.* 2011, **135**, 134104.

[24] F. Castet, E. Bogdan, A. Plaquet, L. Ducasse, B. Champagne, and V. Rodriguez, *J. Chem. Phys.*, 2012, **136**, 024506.

[25] J. Quertinmont, B. Champagne, F. Castet, and M. H. Cardenuto, *J. Phys Chem. A*, 2015, **119**, 5496.

[26] E. Bogdan, A. Plaquet, L. Antonov, V. Rodriguez, L. Ducasse, B. Champagne, F. Castet, *J. Phys. Chem. C*, 2010, **114**, 12760.

[27] T. Seidler, K. Stadnicka, and B. Champagne, *J. Chem. Theory Comput.*, 2014, **10**, 2114.

[28] T. Seidler, K. Stadnicka, and B. Champagne, *J. Chem. Phys*, 2014, **141**, 104109.

[29] T. Seidler, K. Stadnicka, and B. Champagne, *J. Chem. Phys*, 2013 **139**, 114105.

[30] R.J. Bartlett, G. D. Purvis, *Phys. Rev. A*, 1979, **20**, 1313.

[31] E. Perrin, P. N. Prasad, P. Mougenot, and M. Dupuis, *J. Chem. Phys.*, 1989, **91**, 4728.

[32] F. Sim, S. Chin, M. Dupuis, and J. R. Rice, *J. Phys. Chem.*, 1993, **97**, 1158.

[33] H. Sekino, R. J. Bartlett, *J. Chem. Phys.* 1993, **98**, 3022.

[34] D. Jacquemin, B. Champagne, J-M. André, *Int. J. Quantum Chem.*, 1997, **65** 679.

[35] D. Xenides, G. Maroulis, *Chem. Phys. Lett.*, 2000, **319**, 618.

[36] B. Champagne, E. Botek, M. Nakano, T. Nitta, and K. Yamaguchi, *J. Chem. Phys.*, 2005, **122**, 114315.

[37] M. Pecul, F. Pawłowski, P. Jørgensen, A. Köhn, and C. Hättig, *J. Chem. Phys.*, 2006, **124**, 114101.

[38] K. Y. Suponitsky, S. Tafur, and A. E. Masunov, *J. Chem. Phys.*, 2008, **129**, 044109.

[39] J. R. Hammond, K. Kowalski, *J. Chem. Phys.*, 2009, **130**, 194108.

[40] S. L. Sun, G. C. Yang, C. S. Qin, Y. Q. Qui, L. K. Yan, Z. M. Su, and R. S. Wang *Int. J. Quantum. Chem.*, 2010, **110**, 865.

[41] G. Maroulis, M. Menadakis, *Chem. Phys. Lett.*, 2010, **494**, 144.

[42] M. de Wergifosse, B. Champagne, *J. Chem. Phys.*, 2011, **134** 074113.

[43] P. Karamanis, P. Carbonnière, and C. Pouchan, *Chem. Phys. Lett.*, 2011, **135**, 044511.

[44] S. Wouters, P. A. Limacher, D. Van Neck, and P. W. Ayers *J. Chem. Phys.*, 2012, **136** 134110.

[45] T. Helgaker, S. Coriani, P. Jørgensen, K. Kristensen, and K. Ruud, *Chem. Rev.*, **112**, 543.

[46] J. B. Robinson, P. J. Knowles , *J. Chem. Phys.*, 2012, **137** 054301.

[47] J. P. Coe, M. J. Paterson , *J. Chem. Phys.*, 2014, **141** 124118.

[48] M. de Wergifosse, F. Castet, B. Champagne , *J. Chem. Phys.*, 2015, **142** 194102.

[49] F. Sim, D. R. Salahub, and S. Chin, S., *Int. J. Quantum Chem.*, 1992, **43** 463.

[50] J. Guan, P. Duffy, J. T. Carter, D. P. Chong, K. C. Casida, M. E. Casida, M. Wrinn, *J. Chem. Phys.*, 1993, **98** 4753.

[51] D. A. Dixon, B. E. Chase, G. Fitzgerald, N. Matsuzawa, *J. Phys. Chem.*, 1995, **99**, 4486.

[52] S. M. Colwell, N. C. Handy, A. M. Lee, *Phys. Rev. A*, 1996, **53**, 1316.

[53] S. J. A. van Gisbergen, J. G. Snijders, E. J. Baerends, *Phys. Rev. Lett.* 1997, **78**, 3097.

[54] P. Calaminici, K. Jug, A. M. Köster, *J. Chem. Phys.* 1998, **109**, 7756

[55] A. J. Cohen, N. C. Handy, D. J. Tozer, *Chem. Phys. Lett.*, 1999, **303**, 391.

[56] S.J.A. van Gisbergen, P.R.T. Schipper, O.V. Gritsenko, E.J. Baerends, J.G. Snijders, B. Champagne, and B. Kirtman, *Phys. Rev. Lett.*, 1999, **83**, 694.

[57] P. Salek, O. Vahtras, T. Helgaker, and H. Ågren *J. Chem. Phys.*, 2002, **117**, 9630.

[58] M. Kamiya, H. Sekino, T. Tsuneda, and K. Hirao, *J. Chem. Phys.*, 2005, **122**, 234111.

[59] F.A. Bulat, A. Toro-Labbé, B. Champagne, B. Kirtman, and W. Yang, *J. Chem. Phys.* , 2005, **123**, 014319.

[60] D. Jacquemin, E. A. Perpète, M. Medved, G. Scalmani, M. J. Frisch, R. Kobayashi, and C. Adamo, *J. Chem. Phys.*, 2007, **126**, 191108.

[61] B. Kirtman, S. Bonness, A. Ramirez-Solis, B. Champagne, H. Matsumoto, and H. Sekino, *J. Chem. Phys.*, 2008, **128**, 114108.

[62] C.D. Pemmaraju, S. Sanvito, and K. Burke, *Phys. Rev. B*, 2008, **77**, 121204.

[63] T. Körzdörfer, M. Mundt, and S. Kümmel, *Phys. Rev. Lett.*, 2008, **100**, 133004.

[64] R. Armiento, S. Kümmel, T. Korzdorfer, *Phys. Rev. B*, 2008, **77**, 165106.

[65] J. Messud, Z. Wang, P.M. Dinh, P.G. Reinhard, and E. Suraud, *Chem. Phys. Lett.*, 2009, **479**, 300.

[66] F.D. Vila, D.A. Strubbe, Y. Takimoto, X. Andrade, A. Rubio, S.G. Louie, and J.J. Rehr, *J. Chem. Phys.*, 2010, **133**, 034111.

[67] A.V. Arbuznikov, M. Kaupp, *Int. J. Quantum. Chem.*, 2011, **111**, 2625.

[68] H. Sun and J. Autschbach, *ChemPhysChem*, **14**, 2450.

[69] F. Castet and B. Champagne, *J. Chem. Theor. Comput.*, 2012, **8**, 2044.

[70] J. Carmona-Espindola, R. Flores-Moreno, and A.M. Köster, *Int. J. Quantum Chem.*, **112**, 3461.

[71] H. Fukui, Y. Inoue, R. Kishi, Y. Shigeta, B. Champagne, and M. Nakano, *Chem. Phys. Lett.*, 2012, **523**, 60.

[72] I.W. Bulik, R. Zalesny, W. Bartkowiak, J.M. Luis, B. Kirtman, G.E. Scuseria, A. Avramopoulos, H. Reis, and M.G. Papadopoulos, *J. Comput. Chem.*, 2013, **34**, 1775.

[73] S. Nénon, B. Champagne, and M. I. Spassova, *Phys. Chem. Chem. Phys.*, 2014, **16**, 7083.

[74] K. Garrett, X.A. Sosa Vasquez, S.B. Egri, J. Wilmer, L.E. Johnson, B.H. Robinson, and C.M. Isborn, *J. Chem. Theor. Comput.*, **10**, 3821.

[75] J. Carmona-Espíndola, J. L. Gázquez, A. Vela, and S. B. Trickey, *J. Chem. Phys.*, 2015, **142** 054105.

[76] D. L. Silva, R. D. Fonseca, M. G. Vivas, E. Ishow, S. Canuto, C. R. Mendonca, and L. De Boni, *J. Chem. Phys.*, 2015, **142** 064312.

[77] K. Coutinho, R. Rivelino, H. C. Georg, and S. Canuto, *in: Solvation Effects in Molecules and Biomolecules: Computational Methods and Applications*, Springer, p. 159, 2008.

[78] K. Coutinho, S. Canuto, *Adv. Quantum Chem.*, 1997, **28** 89.

[79] K. Coutinho, S. Canuto, and M. Zerner, *J. Chem. Phys.*, 2000, **112** 9874.

[80] M. H. Cardenuto, B. Champagne, *J. Chem. Phys.*, 2014, **141**, 234104.

[81] Allen, M. P. and D. J. Tildesley; *Computer Simulation of Liquids*, Clarendon Press (1987).

[82] W. L. Jørgensen, D. S. Maxwell and Tirado-Rives, J. Am. Chem. Soc. **118**, 11225 (1996).

[83] A. D. Becke, *J. Chem. Phys.*, 1993, **98** 5648.

[84] C. Lee, W. Yang, and R. Parr, *Phys. Rev. B*, 1988, **37** 785.

[85] A. D. Becke, *J. Chem. Phys.*, 1993, **98** 5648.

[86] Y. Zhao, N. E. Schultz, and D. G. Truhlar, *J. Chem. Phys.*, 2005, **123**, 161103.

[87] Y. Zhao, N. E. Schultz, and D. G. Truhlar, *J. Chem. Theory Comput.*, 2006, **2**, 364.

[88] R. Peverati, D. G. Truhlar, *J. Phys. Chem. Lett.*, 2011, **2**, 2810.

[89] T. Yanai, D. Tew, and N. Handy, *Chem. Phys. Lett.*, 2004, **393**, 51.

[90] H. Iikura, T. Tsuneda, T. Yanai, and K. Hirao, *J. Chem. Phys.*, 2001, **115**, 3540.

[91] L. Kronik, T. Stein, S. Refaely-Abramson, and R. Baer *J. Chem. Theor. Comput.*, 2012, **8**, 1515.

[92] J. Autschbach and M. Srebro, *Acc. Chem. Res.*, 2014, **47**, 2592.

[93] H. D. Cohen, C. C. J. Roothaan, *J. Chem. Phys.*, 1965, **43** S34.

[94] M. Wergifosse, V. Liégeois, and B. Champagne, *Int. J. Quantum Chem.*, 2014, **114** 900.

[95] A. A. K. Mohammed, P. A. Limacher, and B. Champagne, *J. Comput. Chem.*, 2013, **34** 1497.

[96] K. Coutinho, H. C. Georg, T. L. Fonseca, V. Ludwig, and S. Canuto, *Chem. Phys. Lett.*, 2007, **437** 148.

[97] K. Coutinho, S. Canuto, DICE (version 2.9): A general Monte Carlo program for liquid simulation, University of São Paulo, (2009).

[98] J. Frisch, et al. Gaussian 09, Revision D01, Gaussian, Inc., Wallingford CT,(2009).

[99] C. M. Breneman and K. B. Wiberg, *J. Comput. Chem.*, 1990, **11**, 361.

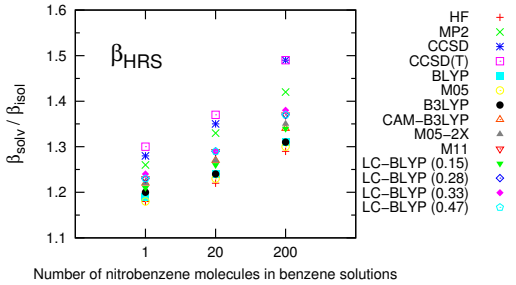

Molecular polarization due to solvation amplifies the impact of electron correlation on the first hyperpolarizability of nitrobenzene.